Structural Characterization of Drug-like Compounds by Ion Mobility Mass Spectrometry: Comparison of Theoretical and Experimentally Derived Nitrogen Collision Cross Sections

ARTICLE *in* ANALYTICAL CHEMISTRY · DECEMBER 2011

Impact Factor: 5.64 · DOI: 10.1021/ac202625t · Source: PubMed

7 AUTHORS, INCLUDING:

Iain Campuzano
Amgen
43 PUBLICATIONS **1,647** CITATIONS
SEE PROFILE

Carol V Robinson
University of Oxford
432 PUBLICATIONS **22,871** CITATIONS
SEE PROFILE

Keith Richardson
Waters Corporation
20 PUBLICATIONS **1,009** CITATIONS
SEE PROFILE

analytical chemistry

Article

pubs.acs.org/ac

Structural Characterization of Drug-like Compounds by Ion Mobility Mass Spectrometry: Comparison of Theoretical and Experimentally Derived Nitrogen Collision Cross Sections

Iain Campuzano,*[,†] Matthew F. Bush,*[,‡] Carol V. Robinson,[§] Claire Beaumont,[∥] Keith Richardson,[⊥] Hyungjun Kim,[#] and Hugh I. Kim[¶]

[†]Amgen, Inc., Department of Molecular Structure, Thousand Oaks, California 91320, United States

[‡]Department of Chemistry, University of Washington, Seattle, Washington 98195, United States

[§]Department of Chemistry, Physical and Theoretical Laboratory, University of Oxford, Oxford, OX1 3QZ, U.K.

[∥]PTS DMPK, GlaxoSmithKline, Ware, Herts, SG12 0DP, U.K.

[⊥]Waters Corporation, MS Technologies Centre, Manchester, M22 5PP, U.K.

[#]Korea Advanced Institute of Science and Technology (KAIST), Daejeon, Korea

[¶]Department of Chemistry, Pohang University of Science and Technology (POSTECH), Pohang, Korea

Supporting Information

ABSTRACT: We present the use of drug-like molecules as a traveling wave (T-wave) ion mobility (IM) calibration sample set, covering the m/z range of 122.1−609.3, the nitrogen collision cross-section (Ω_{N_2}) range of 124.5−254.3 Å^2 and the helium collision cross-section (Ω_{He}) range of 63.0−178.8 Å^2. Absolute Ω_{N_2} and Ω_{He} values for the drug-like calibrants and two diastereomers were measured using a drift-tube instrument with radio frequency (RF) ion confinement. T-wave drift-times for the protonated diastereomers betamethasone and dexamethasone are reproducibly different. Calibration of these drift-times yields T-wave Ω_{N_2} values of 189.4 and 190.4 Å^2, respectively. These results demonstrate the ability of T-wave IM spectrometry to differentiate diastereomers differing in Ω_{N_2} value by only 1 Å^2, even though the resolution of these IM experiments were ∼40 ($\Omega/\Delta\Omega$). Demonstrated through density functional theory optimized geometries and ionic electrostatic surface potential analysis, the small but measurable mobility difference between the two diastereomers is mainly due to short-range van der Waals interactions with the neutral buffer gas and not long-range charge-induced dipole interactions. The experimental RF-confining drift-tube and T-wave Ω_{N_2} values were also evaluated using a nitrogen based trajectory method, optimized for T-wave operating temperature and pressures, incorporating additional scaling factors to the Lennard-Jones potentials. Experimental Ω_{He} values were also compared to the original and optimized helium based trajectory methods.

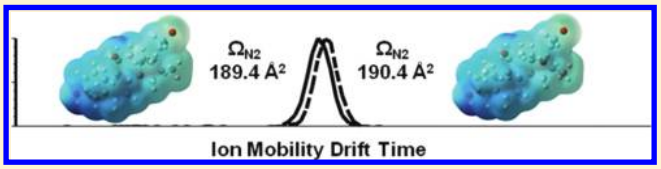

Ion mobility (IM) has the ability to separate rapidly (msec) isomeric species on the basis of differences in their collision cross sections (Ω; physical size and shape) in the gas-phase, as the ion moves through a neutral drift gas, typically helium (He) under the influence of a weak electric field, thus providing specific information on ionic configuration and potential structural confirmation of isobaric species. IM is currently used in many research areas ranging from chemical warfare agent detection,[1] fundamental gas-phase peptide and protein structure determination,[2−5] pharmaceutical compound analysis,[6−8] gas-phase radical cation structure determination,[9] polymer analysis,[10] phospholipid[11] and carbohydrate[12] structural analysis, and more recently, structural biology,[13−16] including mega-Dalton viral capsid analysis.[17]

Mobility measurements have traditionally been performed on drift-tube instrumentation where the mobility of the ion is measured and Ω value derived, using the Mason−Schamp equation.[18] Since the introduction of traveling wave (T-wave) ion mobility (IM) technology in 2004,[19] researchers have typically calibrated those drift-times[11,13,20,21] using drift-tube derived Ω_{He} values.[22] Because of the complex nature of the ion trajectory through the T-wave separator[23] a complete analytical relationship between the ions mobility and the experimental separation parameters has not yet been developed, although initial progress has been made.[24] Recently a collision cross-sectional protein database allowing T-wave calibration in both N_2 and He has been produced.[25] However, such a database does not exist for smaller ionic species, such as pharmaceutically relevant structures. Researchers have begun to investigate, successfully, the separation powers of T-wave IM for a number of low molecular weight isomeric ruthenium anticancer agents,[26,27] position of metabolite hydroxylation,[28] glucoroni-

Received: October 3, 2011
Accepted: December 5, 2011
Published: December 5, 2011

dation,[29] cationic and anionic liquids.[30] In most cases T-wave IM data was acquired with N_2 as the drift-gas, and when the Ω values were calculated, drift-tube derived Ω_{He} values for known tryptic peptides or proteins were used as calibrant species. It has been demonstrated under atmospheric[31] and T-wave operating[32] IM conditions that the use of IM drift gases varying dramatically in polarizability, such as nitrogen (N_2) and carbon dioxide (CO_2), can have a major impact on the IM separation of the ions under investigation, so depending on the species being analyzed, it will be important to choose appropriate calibration compounds[11,25] and use calibrant Ω values that are appropriate for the drift-gas used in the experiment.

Diastereomers are a group of stereoisomers containing more than one stereo center, but not all differing in configuration, therefore, by their very nature, will differ subtly in molecular shape, and in all likelihood, their Ω value. Enantiomers are stereoisomers which differ in configuration at every stereo-center (mirror image) and as demonstrated by the addition of a chiral modifier into the drift gas, chiral IM separation can be achieved at atmospheric working pressures.[33] To date there has been a limited amount of IM research performed on diastereomers using drift-tube,[34−36] high-field asymmetric waveform[37,38] and T-wave[39] IM instrumentation.

To infer ionic structure from IM measurements, experimentally measured Ω values are frequently compared with theoretically derived Ω values, utilizing a model for the interaction between the ion and the buffer gas. Many different theoretical models exist to calculate an ion's mobility in various monatomic (He and argon) and polyatomic drift gases (N_2, carbon dioxide and sulfur hexafluoride), such as the rigid-sphere and the polarization limit,[18,40,41] 12−6−4[41] and 12−4[41−43] potential models and various modified forms thereof.[41,44,45] Other computational approaches calculating collisional integrals describing the ion-neutral interaction are based on the projection approximation,[46−48] exact hard sphere scattering[49] and the trajectory method,[50] which are all based on the ion's interaction with the IM buffer gas He.

Here we present for the first time, the generation of a large and self-consistent set of Ω_{N_2} and Ω_{He} values for a group of drug-like molecules, thus enabling calibration and accurate measurement of T-wave Ω values, notably in N_2 and comparison to an optimized N_2 trajectory method based algorithm. We also investigate the epimeric compounds betamethasone and dexamethasone (Figure 1) differing only in chirality at a single carbon atom, resulting in a subtle, but detectable shape difference, by RF-confining drift-tube IM, T-wave IM, theoretical Ω calculations, and density functional theory (DFT).

EXPERIMENTAL SECTION

A modified Waters Synapt HDMS instrument was used to measure direct Ω values. The T-wave IM device was replaced with a radial RF-only ion confinement, 18 cm long drift-tube, with a linear voltage gradient directing the ions along the axis of transmission to the time-of-flight (ToF) mass analyzer. Direct Ω (N_2 and He) values were determined directly from the slopes of two or more drift-time versus reciprocal drift-voltage plots measured on separate occasions, each of which used ten drift-voltages ranging from 60−200 V in 2.1 Torr N_2 or 2.7 Torr He, and a temperature of 301 ± 1 K measured using 3 T-type thermocouples attached directly to the IM drift-cell. Representative data are shown in Figures S1−S8 (Supporting Information). This instrument and methodology for Ω generation has been described in detail elsewhere.[25]

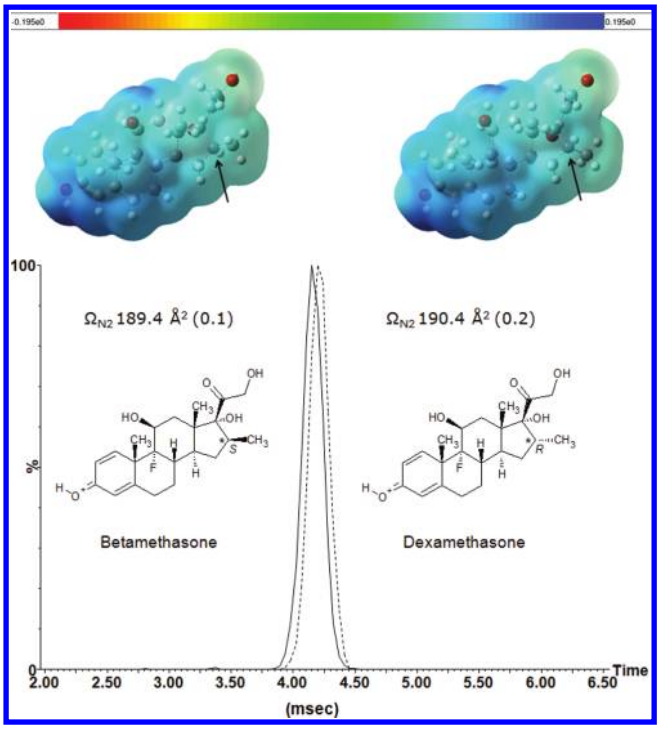

Figure 1. Isosurface depicting B3LYP/6-31G++(d,p) electrostatic potential mapped upon the total electron density for betamethasone and dexamethasone. Isosurface value coloration: blue, positive; red, negative. Arrow indicates the chiral center. T-wave IM analysis of betamethasone and dexamethasone. Displayed are the individual, overlaid ATDs of betamethasone (solid line) and dexamethasone (hashed line). Annotated are the calibrated T-wave measured Ω_{N_2} values. The displayed structures represent the lowest energy protonation site and indicated chiral centers (*). Values in parentheses represent the standard deviation, in percentage, of the T-wave IM measurement.

A mixture of pharmaceutically relevant small molecule compounds, were infused as a mixture through a standard electrospray ion source into the instrument at a concentration of 1 μM (acetonitrile 50% v/v, formic acid 0.1% v/v). The compounds chosen, all singly charged and protonated $[M + H]^+$, were *N*-ethylaniline, acetaminophen, alprenolol, ondansetron, clozapine *N*-oxide, colchicine, verapamil, reserpine, betamethasone, and dexamethasone. All compounds were purchased from Sigma-Aldrich (Poole, Dorset, UK) apart from ondansetron, which was supplied by GlaxoSmithKline (Ware, Herts, UK). Additionally, drift-tube Ω_{N_2} and Ω_{He} values were also obtained for a set of quaternary alkyl ammonium ions (Figures S3, S4, and Table S1, Supporting Information). Errors generated from the slopes of the best fit lines for the ten drift-time versus reciprocal drift-voltage measurements were typically ≤0.6%. Standard deviation of two or more of these experiment sets were typically ≤1.1%. These errors are consistent with those described elsewhere.[25]

Synapt G2 HDMS[51,52] IM analysis was performed at a measured pressure of 3.0 Torr N_2 with T-wave velocities of 500, 475, or 450 m/s and an amplitude of 40 V. T-wave IM calibration was undertaken using the singly charged small molecule ions whose Ω_{N_2} values were derived on the RF-

dx.doi.org/10.1021/ac202625t | *Anal. Chem.* 2012, 84, 1026−1033

confining drift-tube instrument noted above, using a well-documented procedure.[11,13,20,21,25−28,30,51,53−56] Briefly, the drift-tube Ω_{N_2} values were adjusted by multiplying by the square root of the reduced mass and dividing by the charge state of the calibrant species to provide a term that is proportional to the reciprocal mobility of the ion. The measured T-wave arrival-time distributions (ATDs) were corrected for their mass-dependent flight times between the T-wave IM cell and the ToF analyzer. The corrected Ω_{N_2} values were plotted against corrected ATD (msec) values determined using the T-wave separator and the data fitted using an empirically determined power form, $y = ax^n$ (Figure S10, Supporting Information). The derived coefficient n, is obtained from the calibration curve and used to calculate the Ω_{N_2} of betamethasone and dexamethasone from their measured T-wave drift-times obtained under identical operating conditions to those of the calibrant species.

Initial structures for betamethasone and dexamethasone were created through ACDLABS ChemSketch (v12). Five protonation sites were considered. Optimized protonated structures of betamethasone and dexamethasone were generated (Avogadro v1.0.1) at the MMFF94 level of theory using the systematic rotor search option. Structures were first optimized (Gaussian v9) using B3LYP DFT and the 3-21G basis set, then energy minimized using the 6-31G+(d) and 6-31G++(d,p) basis sets. Partial atomic charges were determined using Mulliken, electrostatic surface potential (pop = mk,dipole) and natural population analysis (pop = npa) outputs. Vibrational frequencies and zero-point energies were calculated using the 6-31G++(d,p) basis set. Zero-point corrected energies are reported in Figure S12 (Supporting Information).

Theoretical Ω_{N_2} values[57,58] were calculated using a modified trajectory method. Briefly, the trajectory method[50] was originally developed by Jarrold and co-workers to calculate the theoretical Ω of an ion based on its interaction with the IM buffer gas He. The potential term used in the trajectory method is based on the two body 12−6 potential model:

$$\Phi(\theta, \phi, \gamma, b, r) = 4\epsilon \sum_{i}^{n}\left[\left(\frac{\sigma}{r_i}\right)^{12} - \left(\frac{\sigma}{r_i}\right)^{6}\right] - \frac{\alpha}{2}\left(\frac{ze}{n}\right)^2\left[\left(\sum_{i}^{n}\frac{x_i}{r_i^3}\right)^2 + \left(\sum_{i}^{n}\frac{y_i}{r_i^3}\right)^2 + \left(\sum_{i}^{n}\frac{z_i}{r_i^3}\right)^2\right]$$

The 12 and 6 power terms represent the sum of the two body (ion-neutral) short-range van der Waals interactions; σ is the distance (r) between the centers of mass of each atom of the ionic species and the neutral IM gas (N_2 or He) when the potential minimum becomes positive in value. The expressions θ, ϕ, and γ represent the scattering angles defining the geometry of the ion-neutral collision and b represents the impact factor. The coordinates x_i, y_i, z_i, and r_i are the relative positions of individual atoms with respect to the neutral buffer gas. There is also a term describing the depth of the potential well (ϵ) and a term taking into account the polarizability (α) of the IM buffer gas (He 0.205×10^{-30}m^3; N_2 1.740×10^{-30}m^3), therefore, describing the long-range ion induced-dipole attractive interaction. Additional terms are required to account for the additional interactions between ions and N_2, including the ion-quadrupole interaction and the orientation of the linear N_2 molecule during the neutral collision process of IM separation. For the research described in this manuscript, the authors also added the element fluorine, in addition to further scaling factor modifications which were made to the universal force field atomic energy (ϵ) and van der Waals distance values (σ)[59] used within the N_2 trajectory method algorithm.

Parameters for this modified trajectory method were optimized using RF-confining drift-tube experimental Ω values for a set of compounds obtained from Sigma-Aldrich (Poole, Dorset, UK): *N*-ethylaniline, acetaminophen, tetra-methylammonium, tetra-ethylammonium, choline, acetylcholine (infusion conditions: 1 uM in 49.9% (v/v) acetonitrile/water and 0.1% (v/v) formic acid); naphthalene, phenanthrene, anthracene, pyrene, triphenylene, C_{60} and C_{70}, (infusion conditions: 100% toluene. Operating the electrospray in positive ion mode at a capillary voltage higher than normal ∼4.5 kV, a corona discharge was generated and radical cations [$M^{\bullet+}$] were efficiently generated). The Ω values (both N_2 and He) of the aforementioned molecules were all measured on the RF-confining drift-tube instrument (Figures S5−S8 and Table S2, Supporting Information). Optimized energy minimized coordinate sets were created as described above for betamethasnoe and dexamethasone, with the exception of the $M^{\bullet+}$ radical species naphthalene, phenanthrene, anthracene, pyrene, triphenylene, C_{60} and C_{70}, which were all calculated using B3LYP (unrestricted) and the 6-31G++(d,p) basis set. Additional calculations using the basis set aug-cc-pVTZ were performed for all cation radical structures. No significant difference in theoretical Ω_{N_2} or Ω_{He} values were observed between basis sets 6-31G++(d,p) and aug-cc-pVTZ. Five protonation sites for the geometries of acetaminophen were considered, including tautomeric structures, however only two structures were determined to be energetically favorable (Figure S9, Supporting Information). The theoretical Ω values (both N_2 and He) of both favorable structures were calculated and averaged (Table S2, Supporting Information). All trajectory method calculations were carried out at a simulated temperature of 301 K. The default impact factor (imp; number of points within the Monte Carlo integration of the impact factor and orientation) within the trajectory method was raised from the default value of 25 to 1000, resulting in a total number of 400 000 sampling points and a dramatically improved standard deviation value (≤1.3%) which is comparable with the current RF-confining drift-tube reported errors.

RESULTS AND DISCUSSION

RF-confining drift-tube measured Ω_{N_2} and Ω_{He} values and associated standard deviations are reported in Table 1. Ω_{N_2} values range from 124.5 Å^2 for *N*-ethylaniline to 254.3 Å^2 for reserpine with associated standard deviations values ≤0.6%. Ω_{He} values range from 63.0 Å^2 for *N*-ethylaniline to 178.8 Å^2 for reserpine, and the associated standard deviations for these measurements were ≤0.5%. The drift-tube Ω_{N_2} values for the diastereomer compounds betamethasone and dexamethasone were determined to be 189.6 Å^2 and 190.7 Å^2 respectively and Ω_{He} values for betamethasone and dexamethasone were determined to be 115.1 Å^2 and 116.2 Å^2 respectively. At the analyte concentration (1 μM) under which the N_2 and He RF-

dx.doi.org/10.1021/ac202625t | *Anal. Chem.* 2012, 84, 1026−1033

Table 1. RF-Confining Drift-Tube Derived Ω_{N_2} and Ω_{He} Values for the Drug-like IM Calibration Mix

compound	m/z	Ω_{N_2} (Å^2)[a]	Ω_{He} (Å^2)[a]
N-ethylaniline	122.1	124.5 (0.3)	63.0 (0.4)
acetaminophen	152.1	130.4 (0.6)	67.0 (0.5)
alprenolol	250.2	157.5 (0.5)	96.9 (0.1)
ondansetron	294.2	172.7 (0.4)	105.9 (0.5)
clozapine N-oxide	343.2	180.6 (0.3)	112.5 (0.0)
colchicine	400.2	196.2 (0.3)	130.8 (0.0)
verapamil	455.3	210.0 (0.3)	142.6 (0.1)
reserpine	609.3	254.3 (0.1)	178.8 (0.1)
betamethasone[b]	393.2	189.6 (0.3)	115.1 (0.1)
			121.1[c] (0.2)
dexamethasone[b]	393.2	190.7 (0.0)	116.2 (0.0)
			122.0[c] (0.3)

[a]Values in parentheses represent the standard deviation, in percentage, of the RF-confining IM measurement. [b]Protonated betamethasone and dexamethasone dimers were observed in the He and N_2 IM experiments with measured Ω_{N_2} values of 265.7 Å^2 and 270.8 Å^2 (no standard deviation values were produced because only a single IM experiment was performed) and Ω_{He} values of 186.1 Å^2 (0.1%) and 190.5 Å^2 (0.2%), respectively. Symbols [c]indicate where RF-confining drift-tube Ω_{He} values were used to calibrate T-wave generated ATDs using N_2 as the separator gas.

confining drift-tube measurements were carried out, dimers $(2M + H)^+$ of betamethasone and dexamethasone were also observed, with respective measured and Ω_{N_2} values of 265.7 and 270.8 Å^2 and Ω_{He} values of 186.1 Å^2 and 190.5 Å^2. These dimer Ω_{He} and Ω_{N_2} values can be used to further extend the calibration range over reserpine, on the T-wave instrument when operated in either or N_2 or He. The Ω values of the tetra-alkylammonium, series (from $n = 1$ to $n = 8$) were also determined by RF-confining drift-tube IM in both N_2 (107.4 to 258.3 Å^2) and He (48.5 to 194.0 Å^2; Supplementary Figures S3, S4 and Table S1) all with measured standard deviations ≤0.5%. Our reported Ω_{He} values are highly consistent (≤2.9%) with previously published values[60] which suggests a high degree of consistency between the measured mobilities on the RF-confining drift-tube and uniform electric field (RF-free) drift-tube instrumentation. These tetra-alkylammonium species are not addressed any further within this manuscript.

T-wave IM calibration with N_2 as the drift gas, was performed at three different T-wave velocities, allowing the generation of standard deviation values for T-wave measured Ω_{N_2} values (Figure S10, Supporting Information). Using the first eight compounds noted in Table 1 (*N*-ethylaniline to reserpine), a corrected collision cross-section versus corrected drift-time calibration was performed and used to measure the T-wave Ω_{N_2} values for betamethasone and dexamethasone. Measured T-wave Ω_{N_2} values for betamethasone and dexamethasone were 189.4 and 190.4 Å^2, respectively, (Figure 1) and are in excellent agreement with the RF-confining drift-tube measured Ω_{N_2} values of 189.6 and 190.7 Å^2 (Table 1). It must be noted that in both T-wave and RF-confining drift-tube IM experiments, the diastereomers were infused separately, but these results clearly demonstrate that very subtle ionic conformational differences can be observed and characterized by T-wave IM operating at a modest resolution value. Resolved or partially resolved ATDs would not be obtained at an instrument IM resolution of ~40 ($\Omega/\Delta\Omega$) when the diastereomers were introduced as a mixture. Additionally, we have also used the RF-confining drift-tube derived Ω_{He} values to calibrate the T-wave measured (predominantly in N_2) ATDs of both betamethasone and dexamethasone (Table 1). Interestingly the resultant T-wave derived Ω_{He} values for betamethasone and dexamethasone are 121.1 and 122.0 Å^2, respectively; both 5% higher than the RF-confining drift-tube derived Ω_{He} values reported in Table 1 and also higher than the theoretical trajectory method derived Ω_{He} values reported in Table S2, Supporting Information. On the basis of this evidence, it would appear that using Ω_{He} values to calibrate IM data acquired in N_2 as the T-wave separator gas introduces unnecessary errors.

The development of an N_2 based trajectory method[57,58] is important since it enables the direct comparison of theoretical and measured Ω values of ionic species and the inference of structural information from the ion behavior in gases (N_2) other than the commonly used He. In this particular study T-wave Ω_{N_2} values were generated, since the IM buffer gas used on the T-wave instrument platform is predominantly N_2.[19,51,61] Experimental T-wave Ω_{N_2} values, for a group of phosphatidylcholine structures,[58] based on the Shvartsburg and Smith equations[23] have previously been compared to N_2 based trajectory method Ω values, and demonstrated reasonable (R^2 = 0.91) linearity, but as yet no accurate calibrated T-wave derived Ω_{N_2} values for small molecules have been reported in the literature.

Theoretical Ω_{N_2} and Ω_{He} values were calculated for atomic models of the ions listed in the experimental section (and Table

Table 2. Default and Optimized N_2 and He Trajectory Method Atomic Energy (ϵ; meV) and van der Waals Distance (σ; Å) Parameters for Atoms H, C, N, O, and F

	trajectory method N_2 universal force field		trajectory method N_2 optimized force field		trajectory method He		trajectory method He optimized	
element	ϵ	σ	ϵ	σ	ϵ	σ	ϵ	σ
H	1.9078	2.8860	0.8204	1.2409	0.6500	2.3800	0.6175	2.2610
C	4.5528	3.8510	4.2319	3.5814	1.3400	3.0430	1.3266	3.0126
N	2.9918	3.6600	3.5902	4.3920	1.3400	3.0430	1.4740	3.3473
O	2.6016	3.5000	2.4195	3.2550	1.3400	3.0430	1.0720	2.4344
F	2.1680	3.3640	2.0162	3.1285			1.0720	2.4344
RMS[a]	15.05%		2.63%		4.20%		0.81%	

[a]Reported are the root mean square (RMS) errors of the original and optimized N_2 and He based trajectory method calculated Ω values compared to the RF-confining drift-tube measurements for the tuning compounds in Table S2, Supporting Information. All trajectory method calculations were performed at 301 K.

dx.doi.org/10.1021/ac202625t | *Anal. Chem.* 2012, 84, 1026−1033

S2, Supporting Information) using the trajectory method[50] and a modified form of the trajectory method for calculating mobilities in N_2.[57] Although the theoretically calculated Ω_{He} values agreed reasonably well with corresponding the experimental values (4.2%; Table 2), the theoretically calculated Ω_{N_2} values were significantly larger than the corresponding experimental values (15.05%; Table 2). This suggests that the existing universal force field parameters[59] for calculating mobilities in N_2,[57] which were optimized using compounds possessing a relatively narrow range of Ω_{N_2} values (~85−125 Å^2) that were obtained from mobility measurements at atmospheric pressure and 473 K, may not be appropriate for calculating Ω_{N_2} at the ambient temperatures, low pressures, and broad m/z range of these and many other IM experiments using T-wave and drift-tube instrumental platforms. On the basis of these results, parameters for the N_2 based trajectory method were reoptimized. Analogous to experiments performed by Siu and co-workers[60] on the original He based trajectory method, an additional scaling factor was used to fully optimize the N_2 based trajectory method Lennard-Jones values. This scaling factor was applied to the atomic energy term ϵ (meV) and van der Waals distance term σ (Å) in the potential model noted above. The hydrogen atom atomic energy and van der Waals distance values were scaled by a factor of 0.43, the atoms carbon, oxygen and fluorine atomic energies and van der Waals distances by a factor of 0.93 and the atom nitrogen atomic energy and van der Waals distance by a factor of 1.2. Using these optimized parameters, the theoretical and instrument derived (RF-confining drift-tube) Ω_{N_2} values correlated extremely well (R^2 = 0.9949) over a wide m/z range (tetramethylammonium m/z 74.1 to C_{70} m/z 840.0) and wide Ω_{N_2} range (107−231 Å^2; Figure 2, upper graph) and the RMS values of the optimized N_2 based trajectory method are significantly reduced from 15.05 to 2.63% (Table 2).

Interestingly, the theoretical Ω_{N_2} values for the polycyclic aromatic hydrocarbon (PAH) radical cation structures all appear to be overestimated by the N_2 based trajectory method in comparison to the RF-confining drift-tube derived Ω_{N_2} values (by approximately 5%), even when the hydrogen Lennard-Jones values are scaled (reduced) by 90% or more (carbon Lennard-Jones values are based on the RF-confining drift-tube measured mobilities of C_{60} and C_{70} acquired at 301 K). This would suggest that the optimized N_2 trajectory method does not sufficiently describe the interaction of the planar PAH radical cation structures with N_2, or that the interaction of the PAH radical cations with N_2 in the RF-confining drift-tube is subtly, but measurably different to all other species investigated within this manuscript. These observations are currently under investigation; nevertheless, an excellent linear correlation (R^2 = 0.9949; Figure 2, upper graph) for the entire set of measurements was still achieved. Although the absolute Ω_{N_2} values obtained from RF-confining drift-tube and the trajectory method calculations differ by ~5% for the PAH radical cations, the calculations appear to be sensitive to very small relative differences. For example anthracene and phenanthrene (Figure S11, Supporting Information) are identical in m/z, but have subtly different aromatic ring orientations. The RF-confining drift-tube measurements (in N_2) for anthracene and phenanthrene differ by 0.5 Å^2 and the theoretical Ω_{N_2} values also differ by 0.5 Å^2. These results give us great confidence in the ability of this optimized N_2 trajectory method to detect subtle differences

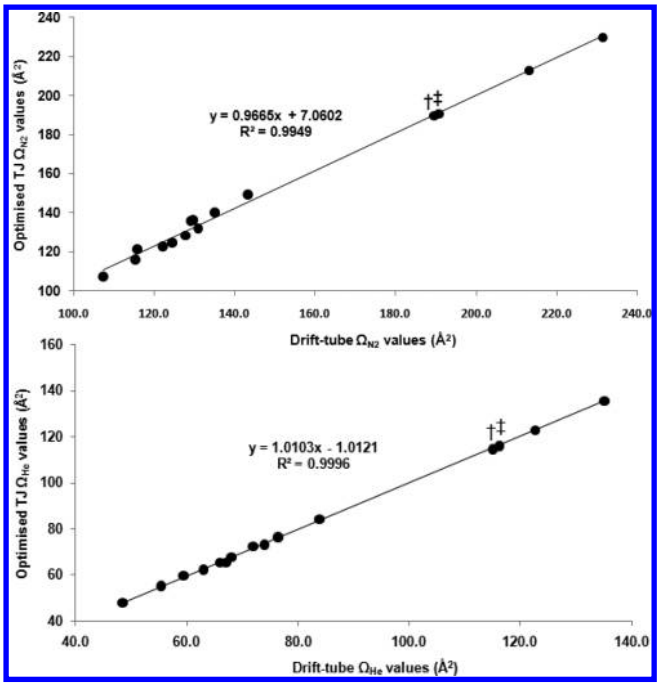

Figure 2. RF-confining drift-tube measured and trajectory method (TJ) calculated Ω_{N_2} (upper) and Ω_{He} (lower) values, using the optimized atomic energy and van der Waals distance values noted in Table 2. Symbols † and ‡ are above the markers for betamethasone and dexamethasone, respectively. DFT optimized geometries of betamethasone and dexamethasone were not used for trajectory method optimization.

in ionic shape, which is further demonstrated in the diastereomers example below.

The atomic energy and van der Waals distances terms ϵ and σ respectively, were also optimized for the He based trajectory method, using the methodology described above. Excellent linear correlation (R^2 = 0.9996; Figure 2, lower graph) was achieved between all theoretical and RF-confining drift-tube measurements for all tuning compounds. It was determined that the level of scaling reported by Siu[60] of 0.92 for all atoms was not required for the He-based trajectory method. Jarrold and co-workers have already demonstrated thorough determination, over a wide temperature and mobility range, of the Lennard-Jones parameters (ϵ 1.34 meV; σ 3.034 Å) for the carbon−He interaction,[50,62] with which we closely agree (Table 2). We do however report significantly scaled values for the atoms H, O, and F (Table 2). The RMS values of the optimized He based trajectory method are significantly reduced from 4.20% to 0.81% (Table 2).

In addition to the atomic coordinates, these Ω_{N_2} and Ω_{He} trajectory method calculations also utilize the partial atomic charge distributions of the ions to calculate the effect of the charge induced dipole effect. Calculations were performed using several methods for calculating the ionic charge distribution. The electrostatic surface potential model implemented in *Gaussian* (version 9.0), which describes partial atomic charge according to the Merz-Singh-Kollman scheme constrained to reproduce the dipole moment (pop = mk,dipole) resulted consistently in a more accurate agreement between theoretical and RF-confining drift-tube measured Ω values (both N_2 and He), than either the Mulliken or natural population analysis partial atomic charge description.

dx.doi.org/10.1021/ac202625t | *Anal. Chem.* 2012, 84, 1026−1033

Betamethasone and dexamethasone have very similar covalent structures (Figure 1). Five protonation sites were considered for their geometries; two carbonyl and three hydroxyl groups (Figure S12, Supporting Information). The DFT zero-point energy calculations indicate that the carbonyl oxygen of the aromatic ring has the greatest proton affinity and structures protonated at this site are lowest-in-energy (most stable) by 1 eV (23 kcal mol^{-1}) and were used for the theoretical Ω calculations. Note that for pharmaceutically relevant molecules,[63,64] an energy cutoff threshold of ≤0.2 eV (5 kcal mol^{-1}) can be considered to be the most favorable site of protonation. The calculated trajectory method Ω_{N_2} values for betamethasone and dexamethasone, protonated at position 1, (Figure S12, Supporting Information) were 189.4 $Å^2$ and 190.4 $Å^2$ respectively (Figure 2, upper and Supporting Information Table S2) and demonstrate excellent agreement with both RF-confining drift-tube (189.6 and 190.7 $Å^2$; Table 1) and T-wave calibrated measurements (189.4 and 190.4 $Å^2$; Figure 1), suggesting that the N_2 based trajectory method is well optimized over a wide range of ionic Ω_{N_2} values and structures, utilizing the scaled Lennard-Jones values. It must be noted that betamethasone and dexamethasone DFT optimized structures were not used to optimize and N_2 (or He) trajectory method Lennard-Jones parameters; they were only used to assess the performance of the optimized N_2 (and He) trajectory method. Since the Synapt G2 instrument was not operated with predominantly He in the T-wave IM separator, we can only compare the betamethasone and dexamethasone RF-confining drift-tube Ω_{He} values with the optimized trajectory method Ω_{He} values. Excellent agreement is observed between the RF-confining drift-tube and optimized trajectory method Ω_{He} values (Figure 2 lower and Table S2, Supporting Information).

The mobility and therefore the calculated Ω value of an ion is a measurement of the sum of the ion-neutral interactions taking place within the separator device of the instrument; a combination of long-range ion-induced dipole interactions and short-range van der Waals interactions between the ion and the neutral buffer gas. If we consider each of these interactions in relation to betamethasone and dexamethasone, we can gain an understanding into the small, but measurable difference in mobility observed in both the RF-confining drift-tube and T-wave IM measurements. Previous studies have indicated that different localizations of charge upon the ion can have a major impact on the ion-neutral interaction.[62,65−67] Figure 1 shows the electrostatic surface potential (B3LYP/6-31G++(d,p)) mapped onto the total electron density of optimized geometries of betamethasone and dexamethasone (individual partial atomic charges are displayed in Figures S13 and S14, Supporting Information). As can be observed, unsurprisingly, the charge distributions of the protonated lowest-energy structures of betamethasone and dexamethasone are almost identical, suggesting that differences in the long-range ion-induced dipole interaction between each diastereoisomer and the neutral N_2 molecule do not significantly contribute to their observed mobility difference. It can therefore be inferred that the small but measurable mobility difference is likely due to the geometric difference in ionic structure, resulting from the single chiral methyl configuration difference (*R* or *S*), which dominates the short-range van der Waals interactions. These observation are consistent with previous IM studies performed on tertiary and quaternary ammonium cations[57] suggesting that the long-range interaction is large (30%) from small ionic structures and decreases to less than 10% as the ionic size increases.

CONCLUSIONS

Using RF-confining drift-tube measured Ω_{N_2} and Ω_{He} values for eight pharmaceutically relevant molecules, a robust and accurate T-wave calibration routine, has been developed, covering the Ω_{N_2} range 124.5−254.3 $Å^2$ and the Ω_{He} range of 63.0−178.8 $Å^2$. Significant progress has also been made optimizing an N_2-based trajectory method algorithm. The application of a scaling factor of 0.93 to universal force field atomic energy and van der Waals distance values for the atoms carbon, oxygen and fluorine, a scaling factor of 1.2 for nitrogen and a scaling factor of 0.43 for hydrogen, within the N_2 trajectory method, results in Lennard-Jones potential values producing theoretical Ω_{N_2} values that are highly consistent with RF-confining drift-tube measured values, over a wide *m*/*z* range and diverse molecule sample set. We also report optimized Ω_{He} trajectory method values tuned on the same diverse sample set. Two reproducibly different T-wave IM ATDs for the diastereomers betamethasone and dexamethasone were also achieved under standard instrument operating conditions. Using the RF-confining drift-tube Ω_{N_2} values as IM calibrants, the T-wave measured Ω_{N_2} values for betamethasone and dexamethasone are accurate to within 0.2% of the RF-confining drift-tube Ω_{N_2} values and the optimized N_2-based trajectory method. We attribute the small, but measurable difference in mobility of betamethasone and dexamethasone a result of the short-range van der Waals interaction of the ion-neutral interaction, and not a long-range charge induced dipole interaction. It is important to note that increased errors on reported Ω values are generated if the T-wave instrument is operated with N_2 as the separator gas and drift-tube derived Ω_{He} values are used for calibration, based on the sample set used in this study. This methodology demonstrates the ability of the current generation of T-wave IM technology to differentiate subtly different ionic structures, both protonated $[M + H]^+$ and radical cation $[M^{\bullet+}]$, some differing in only one chiral center, which are also highly consistent with theoretically derived Ω_{N_2} values.

Importantly, we have generated a small database of Ω_{N_2} values for pharmaceutically relevant compounds, which can be used to calibrate the T-wave IM separator, crucially when operating with N_2 as the IM gas. It is envisioned that this small molecule Ω_{N_2} database and optimized N_2 based trajectory method (and He) will be particularly useful to any group wishing to derive Ω_{N_2} values (and Ω_{He}) of small pharmaceutical-like molecules particularly those measured on a T-wave instrument. For example, identifying sites of metabolic substitutions on drug moieties[28,29] based on the intact molecule, or as recently demonstrated, Ω measurements of substituted fragment ions produced by MS/MS.[68] Additionally, the advantage of the approach we have taken here is that all small molecule calibration compound measurements and algorithm tuning compound measurements were performed on an RF-confining drift-tube instrument with ion optics geometry almost identical to that of the full production T-wave IM separator, on which the small molecule calibration was implemented and optimized trajectory method (both N_2 and He-based) algorithm was evaluated, thus negating an instrument specific ion activation issues. However, it must be noted

dx.doi.org/10.1021/ac202625t | *Anal. Chem.* 2012, 84, 1026−1033

that all RF-confining IM measurements reported in this manuscript were performed at room temperature (301 K) and therefore the N_2-based trajectory method algorithm was optimized for operation at room temperature only. Future temperature dependent RF-confining IM experiments would be appropriate, therefore enabling optimization of the N_2 based trajectory method algorithm over a more comprehensive range of operating temperatures and mobilities, analogous to those performed by Jarrold and co-workers for He.[50,62] Finally, preliminary data has also been obtained on the comparison of theoretically and T-wave generated Ω_{N_2} values of radical peptide cations, which are consistent to ≤4% of Ω_{N_2} of each other, therefore extending the use of the optimized N_2 trajectory method for more than just small molecules.

■ ASSOCIATED CONTENT

Supporting Information

Additional material as described in the text. This material is available free of charge via the Internet at http://pubs.acs.org.

■ AUTHOR INFORMATION

Corresponding Author

*E-mail: iainc@amgen.com (I.C.); bush@chem.washington.edu (M.F.B).

■ ACKNOWLEDGMENTS

The authors would like to thank Paul Schnier (Amgen Inc.) for supporting the research described within this manuscript and Michael Bartberger (Amgen Inc.) for his useful discussions and input into the implementation of DFT described within this manuscript. James Bence and Larry Proctor (Amgen Inc.) are also gratefully acknowledged for their input into automating MOBCAL. Scott Gillingwater (Waters Corp.) is thanked for providing the compounds betamethasone and dexamethasone. MFB was a Waters Research Fellow during the course of this research and CVR is a Royal Society Research Professor.

■ REFERENCES

(1) Steiner, W. E.; Klopsch, S. J.; English, W. A.; Clowers, B. H.; Hill, H. H. *Anal. Chem.* **2005**, *77*, 4792.
(2) Clemmer, D. E.; Hudgins, R. R.; Jarrold, M. F. *J. Am. Chem. Soc.* **1995**, *117*, 10141.
(3) Wyttenbach, T.; von Helden, G.; Bowers, M. T. *J. Am. Chem. Soc.* **1996**, *118*, 8355.
(4) Pierson, N. A.; Valentine, S. J.; Clemmer, D. E. *J. Phys. Chem. B* **2010**, *114*, 7777.
(5) Bleiholder, C.; Dupuis, N. F.; Wyttenbach, T.; Bowers, M. T. *Nat. Chem.* **2011**, *3*, 172.
(6) Chan, E. C.; New, L. S.; Yap, C. W.; Goh, L. T. *Rapid Commun. Mass Spectrom.* **2009**, *23*, 384.
(7) Eckers, C.; Laures, A. M.; Giles, K.; Major, H.; Pringle, S. *Rapid Commun. Mass Spectrom.* **2007**, *21*, 1255.
(8) Bagal, D.; Valliere-Douglass, J. F.; Balland, A.; Schnier, P. D. *Anal. Chem.* **2010**, *82*, 6751.
(9) Momoh, P. O.; Hamid, A. M.; Abrash, S. A.; El-Shall, M. S. *J. Chem. Phys.* **2011**, *134*, 204315.
(10) Bagal, D.; Zhang, H.; Schnier, P. D. *Anal. Chem.* **2008**, *80*, 2408.
(11) Ridenour, W. B.; Kliman, M.; McLean, J. A.; Caprioli, R. M. *Anal. Chem.* **2010**, *82*, 1881.
(12) Fenn, L. S.; McLean, J. A. *Phys. Chem. Chem. Phys.* **2011**, *13*, 2196.
(13) Ruotolo, B. T.; Giles, K.; Campuzano, I.; Sandercock, A. M.; Bateman, R. H.; Robinson, C. V. *Science* **2005**, *310*, 1658.
(14) Sharon, M.; Robinson, C. V. *Annu. Rev. Biochem.* **2007**, *76*, 167.
(15) Taverner, T.; Hernandez, H.; Sharon, M.; Ruotolo, B. T.; Matak-Vinkovic, D.; Devos, D.; Russell, R. B.; Robinson, C. V. *Acc. Chem. Res.* **2008**, *41*, 617.
(16) Smith, D. P.; Radford, S. E.; Ashcroft, A. E. *Proc. Natl. Acad. Sci. U. S. A.* **2010**, *107*, 6794.
(17) Uetrecht, C.; Barbu, I. M.; Shoemaker, G. K.; van Duijn, E.; Heck, A. J. *Nat. Chem.* **2011**, *3*, 126.
(18) Mason, E. A.; McDaniel, E. W. *Transport Properties of Ions in Gases*; Wiley: New York, 1988.
(19) Giles, K.; Pringle, S. D.; Worthington, K. R.; Little, D.; Wildgoose, J. L.; Bateman, R. H. *Rapid Commun. Mass Spectrom.* **2004**, *18*, 2401.
(20) Wildgoose, J. Giles, K. Pringle, S. Koeniger, S. L. Valentine, S. J. Bateman, R. H. Clemmer, D. E. *Proc. 54th ASMS Conf. Mass Spectrom. Appl. Top., Seattle 2006 ThP 64* **2006**.
(21) Ruotolo, B. T.; Benesch, J. L.; Sandercock, A. M.; Hyung, S. J.; Robinson, C. V. *Nat. Protoc.* **2008**, *3*, 1139.
(22) Clemmer, D. E. http://www.indiana.edu/~clemmer/Research/cross%20section%20database/cs%20database.htm.
(23) Shvartsburg, A. A.; Smith, R. D. *Anal. Chem.* **2008**, *80*, 9689.
(24) Giles, K.; Wildgoose, J. L.; Langridge, D. J.; Campuzano, I. *Int. J. Mass Spectrom.* **2010**, *298*, 10.
(25) Bush, M. F.; Hall, Z.; Giles, K.; Hoyes, J.; Robinson, C. V.; Ruotolo, B. T. *Anal. Chem.* **2010**, *82*, 9557.
(26) Williams, J. P.; Bugarcic, T.; Habtemariam, A.; Giles, K.; Campuzano, I.; Rodger, P. M.; Sadler, P. J. *J. Am. Soc. Mass Spectrom.* **2009**, *20*, 1119.
(27) Williams, J. P.; Lough, J. A.; Campuzano, I.; Richardson, K.; Sadler, P. J. *Rapid Commun. Mass Spectrom.* **2009**, *23*, 3563.
(28) Dear, G. J.; Munoz-Muriedas, J.; Beaumont, C.; Roberts, A.; Kirk, J.; Williams, J. P.; Campuzano, I. *Rapid Commun. Mass. Spectrom.* **2010**, *24*, 3157.
(29) Kaur-Atwal, G.; Reynolds, J. C.; Mussell, C.; Champarnaud, E.; Knapman, T. W.; Ashcroft, A. E.; O'Connor, G.; Christie, S. D.; Creaser, C. S. *Analyst* **2011**, *136*, 3911.
(30) Lalli, P. M.; Corilo, Y. E.; de Sa, G. F.; Daroda, R. J.; de Souza, V.; Souza, G. H.; Campuzano, I.; Ebeling, G.; Dupont, J.; Eberlin, M. N. *ChemPhysChem* **2011**, *12*, 1444.
(31) Asbury, G. R.; Hill, H. H. Jr. *Anal. Chem.* **2000**, *72*, 580.
(32) Souza, G. H. M. F.; Campuzano, I. D. G.; Lalli, P. M.; Nachtigall, F. M.; Riccio, M. F.; de Sa, G.; Daroda, R. J.; de Souza, V.; Eberlin, M. N. *Proc. 58th ASMS Conf. Mass Spectrom. Appl. Top., Salt Lake City* **2010**, WP661.
(33) Dwivedi, P.; Wu, C.; Matz, L. M.; Clowers, B. H.; Siems, W. F.; Hill, H. H. Jr. *Anal. Chem.* **2006**, *78*, 8200.
(34) Leavell, M. D.; Gaucher, S. P.; Leary, J. A.; Taraszka, J. A.; Clemmer, D. E. *J. Am. Soc. Mass Spectrom.* **2002**, *13*, 284.
(35) Clowers, B. H.; Dwivedi, P.; Steiner, W. E.; Hill, H. H. Jr.; Bendiak, B. *J. Am. Soc. Mass Spectrom.* **2005**, *16*, 660.
(36) Baker, E. S.; Hong, J. W.; Gidden, J.; Bartholomew, G. P.; Bazan, G. C.; Bowers, M. T. *J. Am. Chem. Soc.* **2004**, *126*, 6255.
(37) McCooeye, M.; Ding, L.; Gardner, G. J.; Fraser, C. A.; Lam, J.; Sturgeon, R. E.; Mester, Z. *Anal. Chem.* **2003**, *75*, 2538.
(38) Guevremenot, R. *J. Chromatogr. A* **2004**, *1058*, 3.
(39) Yamagaki, T.; Sato, A. *Anal. Sci.* **2009**, *25*, 985.
(40) Böhringer, H.; Fahey, D. W.; Lindinger, W.; Howorka, F.; Fehsenfeld, F. C.; Albritton, D. L. *Int. J. Mass Spectrom. Ion Processes* **1987**, *81*, 45.
(41) Steiner, W. E.; English, W. A.; Hill, H. H. Jr. *J. Phys. Chem. A* **2006**, *110*, 1836.
(42) Johnson, P. V. K.; H.I. Beegle, L. W.; Kanik, I. *J. Phys. Chem. A* **2004**, *108*, 5785.
(43) Kim, H. I.; Johnson, P. V.; Beegle, L. W.; Beauchamp, J. L.; Kanik, I. *J. Phys. Chem. A* **2005**, *109*, 7888.
(44) Berant, Z.; Karpas, Z. *J. Am. Chem. Soc.* **1989**, *111*, 3819.
(45) Karpas, Z.; Berant, Z. *J. Phys. Chem.* **1989**, *93*, 3021.
(46) Mack, E. J. *J. Am. Chem. Soc.* **1925**, *47*, 2468.
(47) von Helden, G.; Hsu, M.-T.; Kemper, P. R.; Bowers, M. T. *J. Chem. Phys.* **1991**, *95*, 3835.

(48) Bleiholder, C.; Wyttenbach, T.; Bowers, M. T. *Int. J. Mass Spectrom.* **2011**, DOI: 10.1016/j.ijms.2011.06.014.
(49) Shvartsburg, A. A.; Jarrold, M. F. *Chem. Phys. Lett.* **1996**, *261*, 86.
(50) Mesleh, M. F.; Hunter, J. M.; Shvartsburg, A. A.; Schatz, G. C.; Jarrold, M. F. *J. Phys. Chem.* **1996**, *100*, 16082.
(51) Giles, K.; Williams, J. P.; Campuzano, I. *Rapid Commun. Mass Spectrom.* **2011**, *25*, 1559.
(52) Zhong, Y.; Hyung, S. J.; Ruotolo, B. T. *Analyst* **2011**, *136*, 3534.
(53) Ruotolo, B. T.; Hyung, S. J.; Robinson, P. M.; Giles, K.; Bateman, R. H.; Robinson, C. V. *Angew. Chem., Int. Ed.* **2007**, *46*, 8001.
(54) Leary, J. A.; Schenauer, M. R.; Stefanescu, R.; Andaya, A.; Ruotolo, B. T.; Robinson, C. V.; Thalassinos, K.; Scrivens, J. H.; Sokabe, M.; Hershey, J. W. *J. Am. Soc. Mass Spectrom.* **2009**, *20*, 1699.
(55) Scarff, C. A.; Patel, V. J.; Thalassinos, K.; Scrivens, J. H. *J. Am. Soc. Mass Spectrom.* **2009**, *20*, 625.
(56) Williams, J. P.; Phillips, H. I.; Campuzano, I.; Sadler, P. J. *J. Am. Soc. Mass Spectrom.* **2010**, *21*, 1097.
(57) Kim, H.; Kim, H. I.; Johnson, P. V.; Beegle, L. W.; Beauchamp, J. L.; Goddard, W. A.; Kanik, I. *Anal. Chem.* **2008**, *80*, 1928.
(58) Kim, H. I.; Kim, H.; Pang, E. S.; Ryu, E. K.; Beegle, L. W.; Loo, J. A.; Goddard, W. A.; Kanik, I. *Anal. Chem.* **2009**, *81*, 8289.
(59) Rappe, A. K.; Casewit, C. J.; Colwell, K. S.; Goddard, W. A.; Skiff, W. M. *J. Am. Chem. Soc.* **1992**, *114*, 10024.
(60) Siu, C. K.; Guo, Y.; Saminathan, I. S.; Hopkinson, A. C.; Siu, K. W. *J. Phys. Chem. B* **2010**, *114*, 1204.
(61) Pringle, S. D.; Giles, K.; Wilgoose, J. P.; Williams, J. P.; Slade, S. E.; Thalassinos, K.; Bateman, R. H.; Bowers, M. T.; Scrivens, J. H. *Int. J. Mass Spectrom.* **2007**, *261*, 1.
(62) Shvartsburg, A. A.; Schatz, G. C.; Jarrold, M. F. *J. Chem. Phys.* **1998**, *108*, 2416.
(63) Alex, A.; Harvey, S.; Parsons, T.; Pullen, F. S.; Wright, P.; Riley, J. A. *Rapid Commun. Mass Spectrom.* **2009**, *23*, 2619.
(64) Wright, P.; Alex, A.; Nyaruwata, T.; Parsons, T.; Pullen, F. *Rapid Commun. Mass Spectrom.* **2010**, *24*, 1025.
(65) Counterman, A. E.; Clemmer, D. E. *J. Phys. Chem. B* **2001**, *105*, 8092.
(66) Kaleta, D. T.; Jarrold, M. F. *J. Phys. Chem. A* **2002**, *106*, 9655.
(67) Wu, C.; Siems, W. F.; Klasmeier, J.; Hill, H. H. Jr. *Anal. Chem.* **2000**, *72*, 391.
(68) Cuyckens, F. W.; C. Mortishire-Smith, R. J.; Tresadern, G.; Campuzano, I.; Claereboudt, J. *Rapid Commun. Mass Spectrom.* **2011**, *25*, 3497.

NOTE ADDED AFTER ASAP PUBLICATION

After this paper was published online on December 27, 2011, corrections were made to the equation in the Experimental Section. The revised version was published on January 17, 2012.